doi:10.1093/brain/awm151 *Brain* (2007), **130**, 2715–2724

Cultured muscle cells display defects of mitochondrial myopathy ameliorated by anti-oxidants

Lodovica Vergani,[1] Adriana Malena,[1] Patrizia Sabatelli,[2] Emanuele Loro,[1] Lucia Cavallini,[3] Paolo Magalhaes,[4] Lucia Valente,[1,5] Federica Bragantini,[1] Franco Carrara,[5] Bertrand Leger,[6] Joanna Poulton,[7] Aaron P. Russell[6,8] and Ian J. Holt[9]

[1]Department of Neurological Sciences, University of Padova, 35129 Padova, [2]ITOI-CNR IOP, 40136 Bologna, Departments of [3]Biochemistry and [4]Biomedical Sciences, University of Padova, 35121 Padova, [5]Department of Molecular Neurogenetics, National Neurological Institute C.Besta, 20126 Milano, Italy, [6]Clinique Romande de Readaptation, CH-1951 Sion, Switzerland, [7]Department of Obstetrics and Gynaecology, J Radcliffe Hospital, OX3 9DU Oxford, UK, [8]School of Exercise and Nutrition Sciences, Deakin University, 3125 Australia and [9]MRC-Dunn Human Nutrition Unit, University of Cambridge, CB2 OXY Cambridge, UK

Correspondence to: L. Vergani, c/o Venetian Institute of Molecular Medicine, via Orus, 2; 35129 Padova, Italy
E-mail: lodovica.vergani@unipd.it

The mitochondrial DNA A3243G mutation causes neuromuscular disease. To investigate the muscle-specific pathophysiology of mitochondrial disease, rhabdomyosarcoma transmitochondrial hybrid cells (cybrids) were generated that retain the capacity to differentiate to myotubes. In some cases, striated muscle-like fibres were formed after innervation with rat embryonic spinal cord. Myotubes carrying A3243G mtDNA produced more reactive oxygen species than controls, and had altered glutathione homeostasis. Moreover, A3243G mutant myotubes showed evidence of abnormal mitochondrial distribution, which was associated with down-regulation of three genes involved in mitochondrial morphology, Mfn1, Mfn2 and DRP1. Electron microscopy revealed mitochondria with ultrastructural abnormalities and paracrystalline inclusions. All these features were ameliorated by anti-oxidant treatment, with the exception of the paracrystalline inclusions. These data suggest that rhabdomyosarcoma cybrids are a valid cellular model for studying muscle-specific features of mitochondrial disease and that excess reactive oxygen species production is a significant contributor to mitochondrial dysfunction, which is amenable to anti-oxidant therapy.

Keywords: Cybrids; MELAS; Differentiation; ROS

Abbreviations: cybrids = transmitochondrial hybrid cell; LHON = Leber's Hereditary Optic Neuropathy; MS = clones of cybrids harbouring mutant mtDNA; NARP = Neuropathy, Ataxia and Retinitis Pigmentosa; Opa I = Optic Atrophy I; OXPHOS = oxidative phosphorilation; PBS = phosphate saline buffer; qPCR = quantitative polymerase chain reaction; RD ρ^0 = rhabdomyosarcoma cells without mitochondrial DNA; WT = clones of cybrids with normal (wild type) mitochondrial DNA

Received March 2, 2007. Revised May 10, 2007. Accepted June 6, 2007. Advance Access publication July 11, 2007

Introduction

Mutations in human mitochondrial DNA (mtDNA) are associated with a wide range of human pathologies, as well as being implicated in the normal aging process (Taylor and Turnbull, 2005). One particular mutation, an A to G transition at nucleotide (nt) 3243 in the mitochondrial $tRNA^{Leu(UUR)}$ gene is associated with a broad spectrum of clinical phenotypes, ranging from severe multisystem disorders, such as MELAS (Mitochondrial Encephalomyopathy, Lactic acidosis and Stroke-like episodes) (Goto *et al.*, 1990), to maternally inherited diabetes and deafness (van den Ouweland *et al.*, 1992), cluster headaches, pancreatitis and skeletal myopathy (Moraes *et al.*, 1992).

Cells harbouring A3243G mtDNA display decreased activities of OXPHOS enzyme complexes, in particular Complex I, and as a consequence decreased respiratory capacity (Morgan-Hughes *et al.*, 1995; Dunbar *et al.*, 1996). Several studies focusing on the pathogenic mechanism of the A3243G mutation have demonstrated various structural and functional defects in $tRNA^{Leu(UUR)}$. These include impaired aminoacylation (Chomyn *et al.*, 2000), reduced half-life (Yasukawa *et al.*, 2000) and a reduced steady-state level of the tRNA (Chomyn *et al.*, 2000). The mutant tRNA

adopts an abnormal conformation (Wittenhagen and Kelley, 2002), and there is little or no taurine-modification at the anticodon wobble position in mutated $tRNA^{Leu(UUR)}$, resulting in defective translation (Yasukawa *et al.*, 2005).

A3243G lies within a transcription termination binding site and there is *in vitro* evidence that this can affect termination of the rDNA transcription unit (Hess *et al.*, 1991), however this does not lead to any measurable change in the ratio of rRNA:mRNA *in vivo* (Hammans *et al.*, 1992).

Thus, whilst the A3243G mutation is one of the most extensively studied of the human mitochondrial tRNA mutations, and it is clear that it compromises mitochondrial translation both *in vitro* (Chomyn *et al.*, 1992; Dunbar *et al.*, 1996) and *in vivo* (Morgan-Hughes *et al.*, 1995) due to impaired tRNA function (Yasukawa *et al.*, 2005), it is unclear how a single mutation produces such diverse clinical phenotypes. Tissue-specific factors have been proposed as an explanation but not yet identified in the case of A3243G mtDNA (Jacobs, 2003). The molecular basis of tissue specificity has been explained in two mitochondrial disorders resulting from mutation in nuclear genes, thymidine kinase 2 deficiency (Saada *et al.*, 2003) and a defect in the mitochondrial translation machinery (Antonicka *et al.*, 2006).

The electron transport chain (ETC) is the main source of cellular reactive oxygen species (ROS). Complexes I and III generate superoxide anion radicals as a by-product of electron transport. The amount of ROS is dependent on the tissue and its mitochondrial activity. Most free radicals are neutralized by the antioxidant defense system, but if this is compromised or overwhelmed damage to protein, lipid and DNA will ensue. Some ROS are required for intracellular signalling, cell proliferation, differentiation apoptosis and senescence (Finkel, 2003), and so it is not desirable to ablate ROS entirely. Several mtDNA mutations, including A3243G, and neurodegenerative diseases have been associated with increased ROS production (Kirkinezos and Moraes, 2001). However the contribution of ROS to pathogenesis and diverse clinical features is unclear.

With the aim of understanding the pathogenic mechanism of A3243G and other mtDNA mutations, we generated a ρ^0 cell line derived from muscle, rhabdomyosarcoma or RD ρ^0 cells. This cell line expresses muscle specific isoenzymes and retains the ability to terminally differentiate to multinuclear myotubes, which can be innervated (Vergani *et al.*, 2000). In this study, mitochondria from fibroblasts of MELAS patients or controls were transferred to RD ρ^0 cells. Differentiation and innervation were performed enabling the effects of the A3243G mutation to be studied during *in vitro* muscle developmental, and in electrophysiologically active cells, where the demand for mitochondrial function is expected to be considerably higher than in undifferentiated cells. Analyses of ROS production and ROS defense in the presence and absence of an anti-oxidant, *N*-acetyl cysteine (NAC), suggest a direct link between mitochondrial abnormalities and elevated ROS production. Because ROS damage appears to be a significant component of mitochondrial myopathy anti-oxidants may prove an effective treatment for the muscular pathology of MELAS, and other mitochondrial OXPHOS disorders.

Methods

Transmitochondrial cell lines

A human ρ^0 rhabdomyosarcoma cell line (RD ρ^0) (Vergani *et al.*, 2000), lacking mtDNA, was used to generate transmitochondrial cell lines, or cybrids (King and Attardi, 1989). Four cybrids contained 100% wild-type mtDNA (WT2, WT4, WT6 and WT7) from four normal healthy subjects, as described (King and Attardi, 1989). Another four cybrids (MS3, MS4, MS5 and MS6), harboured 99% A3243G mtDNA, derived from 55% mutant mtDNA fibroblasts (data not shown) of a 42-year-old Italian male with MELAS. He presented with MELAS symptoms and bilateral hearing loss, vomiting, diarrhoea and abdominal pain, the patient died 4 years later. No other mtDNA mutations were present in MS6 and WT7 clones, based on sequencing their entire mtDNA (Supplementary Table 1). The proportion of A3243G mtDNA in WT7 and MS6 RD cybrids was analysed by last cycle PCR at intervals and did not alter throughout the study (Supplementary Fig. 1d).

Cell cultures, differentiation and innervation with fetal rat spinal cord

Prior to fusion, undifferentiated cybrids were grown in Dulbecco's modified Eagle's medium (4500 mg glucose/l, 110 mg pyruvate/l), supplemented with 10% fetal bovine serum (FBS) and antibiotics. For muscle differentiation, WT and A3243G mutated RD cybrids were seeded in this medium at a density of 5 and 7×10^3 cells per cm^2, respectively. After 2 days, the medium was replaced with differentiating medium (F14 medium (Seromed, Germany), 2% FBS, 100 nM 12-*0*-tetradecanoylphorbol-13-acetate (TPA), 10 µg/ml insulin, penicillin, streptomycin and amphotericin B). Myotube formation occurred spontaneously 6–7 days later for WT RD cybrids and after 7–9 days for mutated RD cybrids. In some experiments, aneural myotubes (differentiated) cultured WT and MS RD-cybrids, fed for 4 days with differentiation medium, were innervated by fetal rat spinal cord as previously described (Kobayashi *et al.*, 1987). Briefly, explants of spinal cord with dorsal root ganglia attached from 13-day-old fetuses of Sprague–Dawley rats were placed on the top of cybrid cells (Supplementary Fig. 2a and e). Innervated cells were fed with differentiated medium w/o TPA for 15–20 days (Supplementary Fig. 2b–d, f–h). Muscle differentiation was confirmed by qPCR detection of the muscle-specific isoenzyme creatine kinase (M-CK) (Supplementary Fig. 2i), and by the presence of fetal myosin, based on immunohistochemistry (Supplementary Fig. 2l and m).

Morphological analysis

Morphological detection of ROS production was carried out in living cells using 2′,7′-dichlorofluorescin-diacetate (H_2-DCF-DA). Cells on a coverglass were loaded with 3 µM H_2-DCF-DA and 125 nM Mitotracker red (Mit red, Ex: 488 nm; Em: 578 nm) in the growth medium for 30' at 37°C, rinsed twice with warm PBS and observed in PBS. Deacetylation and oxidation of H_2-DCF-DA

yields the fluorescent product 2′,7′-dichlorofluorescin, or DCF (Ex : 488 nm; Em : 525 nm), which was detected by confocal microscopy (Nikon Eclipse E600 microscope equipped with a Biorad MRC-1024 laser scanning confocal imaging system). Cytochrome *c* oxidase (COX) and succinate dehydrogenase (SDH) activity was visualized cytochemically in cell cultures grown on coverglass as described (Tiranti *et al*., 1995). The mitochondrial network of living cells was stained with 125 nM Mitotracker red (Molecular Probes). In undifferentiated and differentiated RD cybrids mitochondrial distribution were quantified as fluorescence signal (arbitrary unit) plotted against the distance from nucleus (pixel) using IMAGE software.

Transmission electron microscopy

RD cybrids were fixed with 2.5% glutaraldehyde in 0.1 M cacodylate buffer (pH 7.4), post-fixed with 1% osmium tetroxide after an extensive washing in 0.1 M cacodilate buffer (pH 7.4), and dehydrated in graded alcohol. Monolayers were detached by rapid washing with propylene oxide, centrifugated and embedded in Epon 812 resin. Ultrathin sections, stained with uranyl acetate and lead citrate, were observed in a Philips EM400 electron microscope at 120 kv. About a hundred cells were analysed for each cell line. In differentiated samples, myotubes were distinguished from resting cells on the basis of the presence of several nuclei or well-organized myofibrils.

Biochemical assays

Glutathione and oxidized glutathione amounts were measured enzymatically by the determination of the chromophoric product 2-nitro-5-thiobenzoic acid, as previously described (Vergani *et al*., 2004). GSH peroxidase (GPX), reductase (GR) and catalase activities were measured in the clear supernatant fraction, 105 000 g_{max} for 30 min, of total cell lysate as previously described (Vergani *et al*., 2004). Oxygen consumption by intact cells was measured with an YSI 5300 oxymeter (YSI Inc., Yellow Springs, OH-USA) on samples contained $3–5 \times 10^6$ cells in 2 ml DMEM lacking glucose and supplemented with pyruvate and 5% dialysed FBS. Evaluations were done at least in triplicate for each cell line.

Detection of ROS production

The rate of H_2O_2 formation in living cells was determined using the oxidation in the extracellular medium of 20 μM fluorogenic indicator amplex red in the presence of 1 unit/ml horseradish peroxidase (POD) and expressed as pmol/min/mg prot. Fluorescence was recorded in a microplate reader (1420 Victor2, Perkin Elmer Life Science-USA) (Ex: 530 nm; Em: 585 nm), in presence of 10 μM apocynin (4′-hydroxy-3′-methoxyacetophenone) that inhibits H_2O_2 produced by plasma membrane NADPH oxidase. In a typical experiment, cells growing in a 12 well-plate, were incubated with 10 μM apocynin for 20' in F14, 2% FCS w/o TPA at 37°C. The first measurement, taken immediately after addition of reactants, was designated background fluorescence. The fluorescent signal of the central area of the well was recorded every 10 min for 30–90 min.

Reverse transcription and quantitative PCR

Five micrograms of RNA was reverse transcribed to cDNA using random hexamers and the Stratascript enzyme. Quantitative PCR was performed using an MX3000p thermal cycler system and Brilliant® SYBER Green QPCR Master Mix, as described (Leger *et al*., 2006). The PCR conditions for all genes consisted of one cycle at 90°C for 2 min, followed by 45 cycles consisting of 95°C for 15 s, annealing and prolongation at 60°C for 60 s. The primer sequences are listed in Supplementary Table 2.

Statistical analysis

Data were expressed as mean ± SD. Statistical analysis of group differences was examined using Student's *t*-test. The differences were considered significant at the 95% confidence level ($P < 0.05$).

Results

Redox homeostasis is perturbed in differentiated RD cybrids carrying mutant mtDNA

In order to evaluate ROS homeostasis during muscle development in RD cybrids harbouring A3243G mutant mtDNA, cells were incubated with the intracellular ROS-sensitive fluorescent probe dichlorofluorescein (DCF) diacetate. In undifferentiated RD cybrids there was no difference in DCF signal between cells with wild-type and A3243G mtDNA (Fig. 1a). In contrast, differentiated myotubes with A3243G mtDNA (MS3 and MS6) produced a stronger DCF signal than controls (WT2, WT6, WT7) (Fig. 1a). To evaluate the effect of an antioxidant, the same cell lines were treated with 0.5 mM *N*-acetylcysteine (NAC) during differentiation, a period of 7–9 days. NAC is a thiol agent and a precursor of GSH synthesis; it is moreover a source of sulphydryl groups in cells and scavenges free radicals (Kelly, 1998). NAC treatment decreased the DCF fluorescence in myotubes with A3243G mtDNA (M3, MS6) (Fig. 1a). Another measure of ROS homeostasis was provided by assaying hydrogen peroxide levels using amplex red (Van Heerebeek *et al*., 2002). The rate of release of H_2O_2 was concordant with the DCF results, as H_2O_2 production doubled ($P < 0.001$) after differentiation of A3243G RD cybrids, yet was near normal when the same cells were incubated with NAC during differentiation (Fig. 1b). There was no such increase in H_2O_2 when RD cybrids without A3243G mtDNA (WT2, WT6 and WT7) differentiated to form myotubes (Fig. 1b).

The steady-state level of intracellular ROS depends on the balance between the rates of ROS generation and detoxification. Glutathione (GSH), a key component of the antioxidant defense system, is oxidized to glutathione disulphide (GSSG) in the presence of ROS, and GSSG is subsequently secreted from the cell. Hence, GSH is involved in maintaining cellular redox balance and in protecting against oxidative damage, and the GSH^2/GSSG ratio is a good indicator of cellular redox state (Schafer and Buettner, 2001). The level of GSH was marginally lower in undifferentiated cybrids with A3243G mtDNA compared to controls, whilst that of GSSG was slightly raised (Fig. 2a and b), which is suggestive of increased yet tolerable oxidative stress, in light of the low steady-state level of ROS

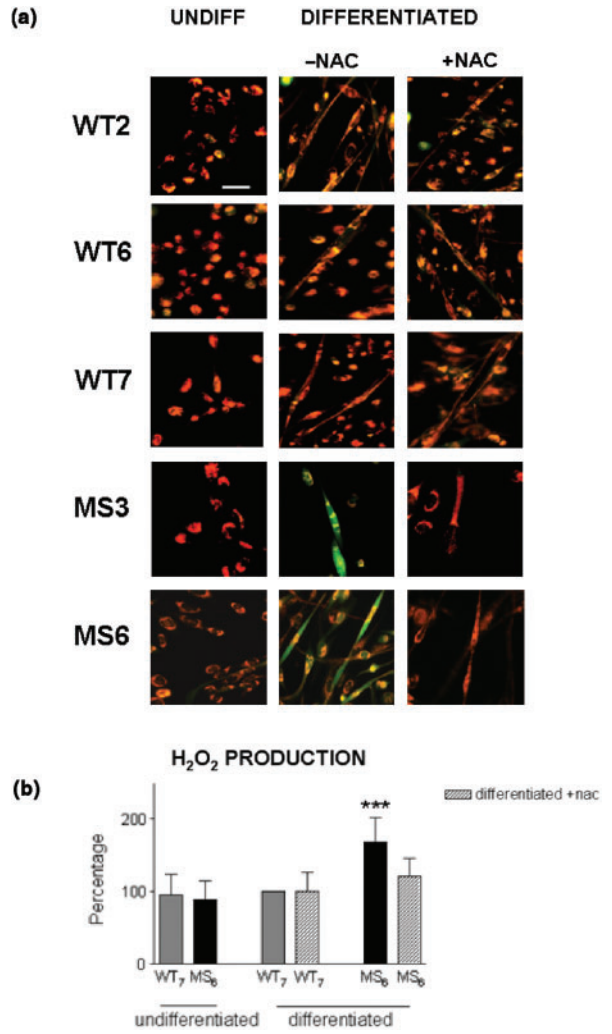

Fig. 1 ROS production in differentiated myotubes with A3243G mtDNA. (**a**) DCF oxidation in undifferentiated (UNDIFF) RD cybrids and in 7–9 days differentiated RD myotubes. Green/yellow signal is indicative of DCF oxidation. Red signal corresponds to the mitochondrial network. Differentiated wild type and mutant cybrids were treated for almost 7 days with 0.5 mM NAC = methods. RD cybrids without A3243G mtDNA, clone 2 (WT2), clone 6 (WT6) and clone 7 (WT7); A3243G RD cybrids, clone 3 (MS3) and clone 6 (MS6). (**b**) H_2O_2 measurement in undifferentiated RD cybrids and in 7–9 days differentiated RD myotubes. Cells were incubated with amplex red and horseradish peroxidase in presence of NADH oxidase inhibitor apocynin, see 'Methods' section. Red fluorescent signal (ex 530 nm—em 590 nm) was recorded for 30 min. H_2O_2 production was expressed as percentage of the basal value (100%) obtained in differentiated WT7 RD cybrids. Basal value was 135 ± 40 pmol/min/mg protein and was obtained in six independent experiments, with three or six samples per experiment. Data represent mean ± SD of three experiments performed with three or six samples. Significant difference from control: $^{***}P < 0.001$. Scale bar: **a**, 20 μm.

(Fig. 1a and b). In A3243G-containing RD cybrids, differentiation triggered a substantial fall in GSH concentration (Fig. 2a). Undifferentiated A3243G RD cybrids had a slightly more oxidized redox state than wild-type cybrids, based on the GSH^2/GSSG values (Fig. 2c) and this difference was much more pronounced after differentiation (Fig. 2c). Differentiation of control cells halved GSH^2/GSSG (Fig. 2c), suggesting that oxidative stress is intrinsic to muscle differentiation, and not merely an effect seen in cells with high levels of mutant mtDNA. Incubation of A3243G RD cybrids with 0.5 mM NAC throughout the differentiation period (7–9 days) was associated with a doubling (170–260%) of cellular GSH content (Fig. 2a) and four 10-fold increase in GSH^2/GSSG compare to untreated cells (Fig. 2c).

The GSH pool is regulated by glutathione reductase (GR) and glutathione peroxidase (GPx). Both enzymes play important roles in antioxidant defense, because GR reduces GSSG to GSH and GPx converts H_2O_2 to H_2O, by coupling the oxidation of GSH to GSSG. GR and GPx activities increased significantly in the one differentiated A3243G RD cybrid tested (Fig. 2d and e) albeit to differing extents (~6 fold and 2 fold, respectively). Catalase activity was a little higher in the undifferentiated RD cybrid with mutant mtDNA but this did not increase further upon differentiation (Fig. 2f). NAC treatment had no appreciable effect on the activity of GR, GPx or catalase (Fig. 2e and f).

Mitochondrial dysfunction and form in differentiated RD cybrids with A3243G mtDNA

Differentiation from myoblasts to myotubes involves a shift from glycolysis to oxidative phosphorylation as the major source of ATP (Leary *et al.*, 1998; Lyons *et al.*, 2004). These changes in energy metabolism are associated with increased mitochondrial biogenesis and mitochondrial redistribution (Kraft *et al.*, 2006). Therefore the morphology and function of mitochondria in undifferentiated and differentiated RD cybrids with A3243G was analysed. *In vivo* A3243G mtDNA is associated with decreased COX activity and increased SDH activity; indeed these are hallmarks of mitochondrial myopathy. In earlier cell models with A3243G mtDNA, which all involved rapidly proliferating cells, COX was also decreased, whereas SDH was unaltered (Dunbar *et al.*, 1995). Undifferentiated RD cybrids with A3243G mtDNA were superficially similar to other proliferating cybrids; however, they had 70–90% decreased oxygen consumption compared to WT clones (Supplementary Fig. 1a) and histochemical stains for COX (data not shown) and SDH indicated that the former activity was impaired, whereas SDH staining was indistinguishable from controls (Supplementary Fig. 1b, SDH). In contrast, RD myotubes with mutant mtDNA (MS6) had increased SDH staining, particularly around the nucleus (Fig. 3a, SDH), in addition to decreased COX activity (Fig. 3a, COX). SDH staining was similar to controls when 0.5 mM NAC was added to the growth medium during the formation of myotubes with A3243G mtDNA (Fig. 3a, SDH). Aberrant mitochondrial distribution associated with A3243G mtDNA was still more pronounced in innervated myotubes (Fig. 3a, Mit red). Innervated cybrid myotubes with wild-type mtDNA

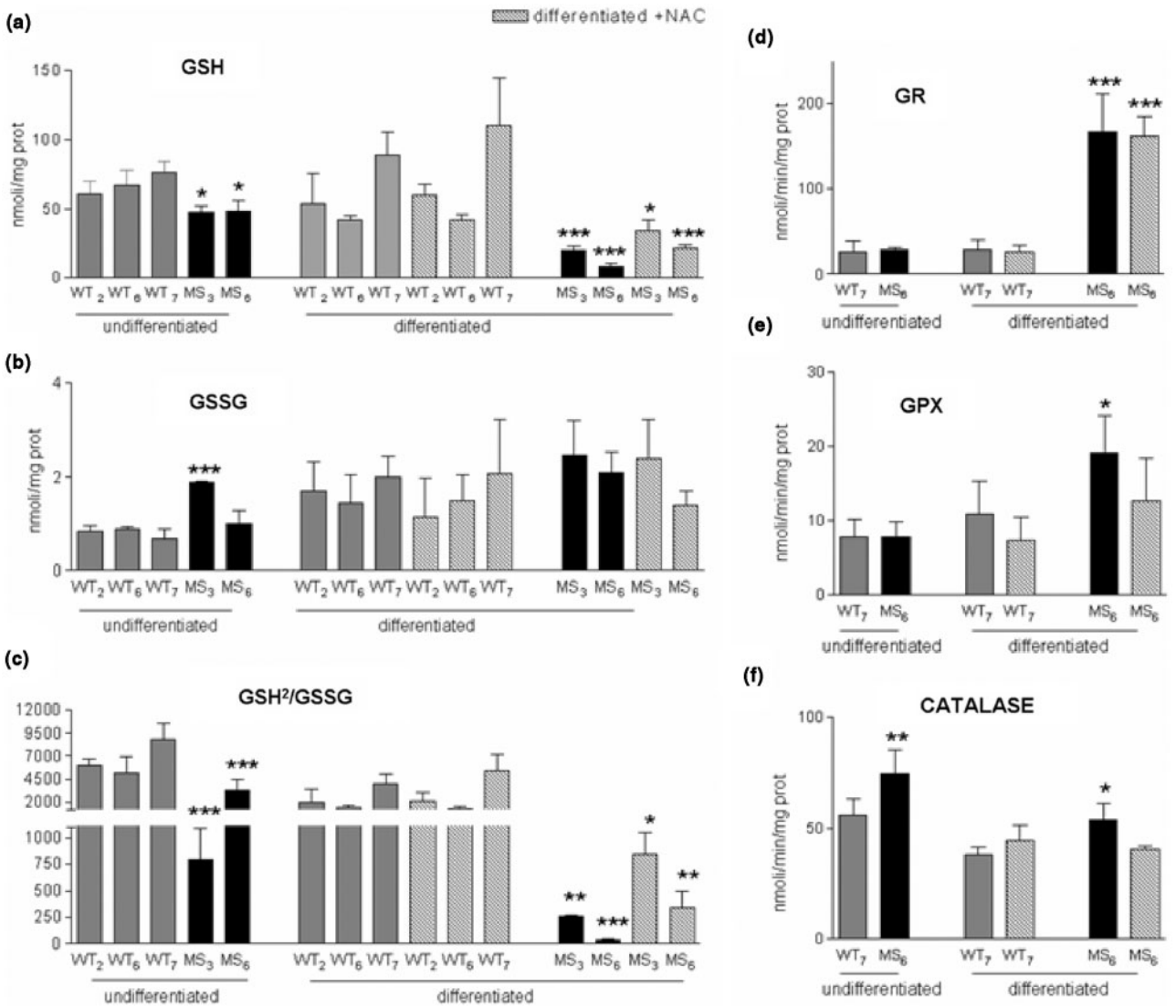

Fig. 2 Antioxidant defences in undifferentiated RD cybrids and in differentiated RD myotubes. RD cybrids without A3243G mtDNA (WT2, WT6 and WT7) and in A3243G RD cybrids (MS3 and MS6). (**a**) GSH concentration, nmol/mg protein [**undiff* MS3 and MS6 versus *undiff* WT2, WT6, WT7]; [****diff –NAC* MS3 and MS6 versus *diff –NAC* WT2, WT6, WT7]; [**diff* + *NAC* MS3 versus *diff –NAC* MS3]; [****diff* + *NAC* MS6 versus *diff –NAC* MS6] (**b**) GSSG concentration, nmol/mg protein [****undiff* MS3 versus *undiff* WT2, WT6, WT7] (**c**) ratio of GSH^2/GSSG [****undiff* MS3 and MS6 versus *undiff* WT2, WT6, WT7]; [***diff* MS3 versus *diff* WT2, WT6, WT7]; [****diff* MS6 versus *diff* WT2, WT6, WT7]; [**diff* + *NAC* MS3 versus *diff –NAC* MS3]; [***diff* + *NAC* MS6 versus *diff –NAC* MS6]. Values are expressed as mean ± SD of at least three assays carried out in duplicate. (**d**) Glutathione reductase activity (GR) [****diff* ± *NAC* MS6 versus *diff* ± *NAC* WT7] (**e**) glutathione peroxidase activity (GPx) [* *diff* MS6 versus *diff* WT7] (**f**) catalase activity [***undiff* MS6 versus *undiff* WT7] [**diff* MS6 versus *diff* WT7]. Values are expressed as mean ± SD of at least three assays carried out in duplicate, units are nmol/min/mg protein. Significant differences: $^{*}P < 0.05$; $^{**}P < 0.01$; $^{***}P < 0.001$.

had thread-like mitochondria scattered throughout the cytoplasm, whereas mitochondria of innervated myotubes with A3243G mtDNA were clustered around the nucleus (Fig. 3a, Mit red). The visual impression of altered mitochondrial distribution in myotubes with A3243G mtDNA was corroborated by a quantitative analysis of mitochondrial distribution. The fluorescent signal, corresponding to mitochondria, when plotted against the distance from the nucleus, revealed a marked decrease in mitochondrial signal in A3243G RD myotubes compared to controls (Fig. 3b). When treated with NAC the mitochondria of innervated A3243G myotubes had the thread-like appearance and distribution of control innervated myotubes [Fig. 3a (Mit red) and b].

Transmission electron microscopy revealed pronounced ultrastructural changes in the mitochondria of A3243G RD myotubes, compared to control myotubes. Myotubes with A3243G mtDNA had swollen, rounded mitochondria, with fewer cristae than normal (Fig. 4g and h). Myofibrils with mutant mtDNA also had paracrystalline inclusions in many mitochondria, however there were no detectable highly condensed mitochondria, which are indicative of

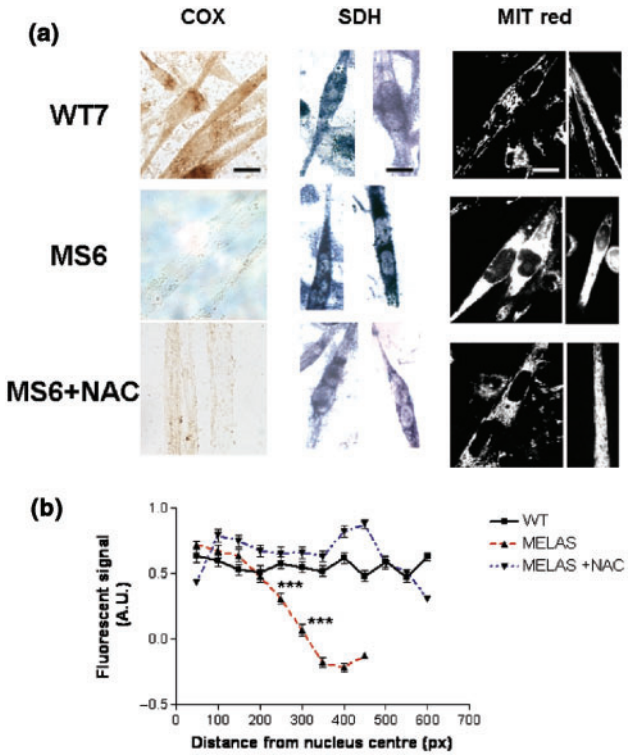

Fig. 3 Altered mitochondrial distribution in myotubes with A3243G mtDNA is prevented by NAC treatment. (**a**) COX histochemical staining of RD myotubes was positive in RD myotubes without A3243G mtDNA (WT7) and negative in differentiated RD cybrids with A3243G (MS6) irrespective of the presence of NAC. SDH staining produced an increased signal in the perinuclear zone of MS6 myotubes but not in WT7 myotubes. Treatment with the antioxidant NAC (0.5 mM) averted the increased staining in MS6 RD cybrid myotubes, rendering them indistinguishable from WT7 RD cybrids. Mitotracker red (MIT red) loaded mitochondria of innervated RD cybrids visualised by confocal microscopy. Innervated MS6 RD myotubes had mitochondria concentrated in the perinuclear region. Chronic antioxidant treatment with NAC (0.5 mM for 15 days) resulted in a normal mitochondrial distribution. There was no difference in the shape or distribution of mitochondria in undifferentiated RD cybrids with or without mutant mtDNA (Supplementary Fig. 1b and c). (**b**) The quantification of mitochondrial distribution in 11 days innervated RD myotubes was obtained as fluorescence signal, expressed in arbitrary units, plotted against the distance from nucleus (pixel; 1 μm: 10 pixels). The values of each point of differentiated cells were mean ± SD of 37 measurements in WT7 and 37 measurement in MS6 RD cybrid myotubes w/o NAC and 20 measurements in MS6 RD myotubes after NAC treatment. The difference between innervated fibres with and without A3243G mtDNA WT and MS was significant ($P < 0.001$), as was the difference between A3243G containing fibres supplemented with and without NAC ($P < 0.001$). Scale bar: **a**, 20 μm.

dead mitochondria, so-called mitoptosis (Pletjushkina *et al.*, 2006) (Fig. 4g and h). Here again, NAC treatment of differentiated A3243G RD myotubes restored mitochondria to normal based on electron microscopy, although the formation of paracrystalline inclusions persisted (Fig. 4i–l, insert). The underlying defect in OXPHOS was also unaffected by NAC treatment (Fig. 3a, COX).

Mitochondrial morphology, movement and distribution depends on Mitofusin 1 (Mfn1), Mitofusin 2 (Mfn2), dynamin-related protein 1 (Drp1) and Opa 1, among others (Chan, 2006). To determine whether the abnormal mitochondrial distribution in A3243G myotubes described above was correlated with the expression of these genes, RNA was isolated and quantified by real-time PCR. In control RD myotubes, Mfn1 and Mfn2 mRNA doubled after differentiation (Fig. 5a and b), in line with an earlier report (Bach *et al.*, 2003), whereas Mfn1 and Mfn2 expression fell in A3243G RD myotubes (Fig. 5a and b). These changes are commensurate with increased ROS production, as NAC treatment once again produced a profile much more like control RD myotubes. More modest, yet similar, changes in DRP1 expression were observed (Fig. 5c), but there was no significant change in OPA1 mRNA levels (Fig. 5d).

Discussion

This study demonstrates that terminally differentiated and innervated RD cybrids are a valid cellular model for studying muscle-specific features of mitochondrial disease. Proliferating cells are heavily dependent on glycolysis for ATP production and so are expected to be less reliant on oxidative phosphorylation than, for example, mature muscle. Differentiated RD cybrids with A3243G mtDNA developed features of diseased muscle: there was elevated ROS production, abnormal mitochondrial distribution and deposition of paracrystalline inclusions. All but the last of these was prevented by anti-oxidant treatment.

Under normal conditions the potentially damaging effects of ROS are limited by a variety of antioxidants. Undifferentiated RD cybrids carrying A3243G mtDNA were for the most part indistinguishable from controls, however, after forming myotubes there was a considerable increase in oxidative stress, based on the high DCF signal and raised H_2O_2 production (Fig. 1a and b). The absolute level of ROS production in A3243G containing myotubes was almost certainly higher than these measurements imply, as depleted stocks of GSH and raised GPx activity indicate that the tripeptide has been consumed in an effort to contain ROS (Fig. 2a and e), which suggests that the antioxidant defence system is close to being overwhelmed in such cells. Oxidative stress is expected to increase after differentiation *in vivo* as muscle is more reliant on aerobic ATP production than proliferating cells, which tend to be highly glycolytic; this effect is exacerbated by impaired mitochondrial function (Chomyn *et al.*, 1992). The data are therefore consistent with the notion that the increase in oxidative stress associated with MELAS mitochondria exceeds a critical threshold in differentiated muscle, and thereby offers a rational explanation for the tissue-specific features of this and many other mitochondrial diseases.

The oxidative stress observed may be due, at least in part, to the culture conditions (Halliwell, 2003), however, this

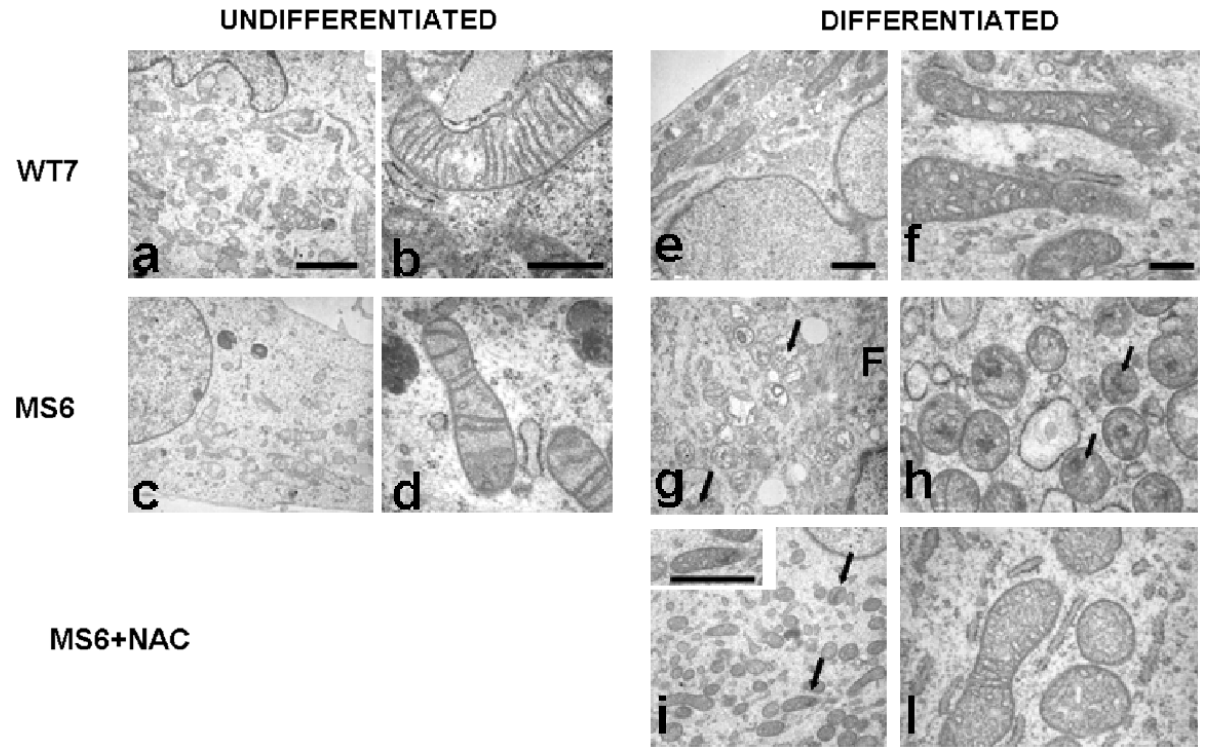

Fig. 4 The abnormal ultrastructural of mitochondria in myotubes with A3243G mtDNA responds to anti-oxidant treatment. (**a–d**) Mitochondria of undifferentiated RD cybrids. (**c, d**) Undifferentiated cybrids with A3243G mtDNA (MS6) were indistinguishable from normal RD cybrids (WT7) (**a, b**) in overall aspect and in cristae shape. (**a, c**) TEM low magnification. (**b, d**) TEM high magnification. (**e–l**) Mitochondria of differentiated RD cybrids. (**g, h**) Mitochondria in myotubes with A3243G mtDNA appeared swollen, with paracrystalline inclusions (arrows). F: well-defined actin–myosin filaments. The analysis was performed only in cells with polynuclei or well-organized myofibrils. (**i–l**) NAC treated MS6 RD cybrids. Scale bars: **a** and **c**, 200 nm; **b** and **d**, 100 nm; **e, g** and **i**, 500 nm; **f, h** and **l**, 100 nm.

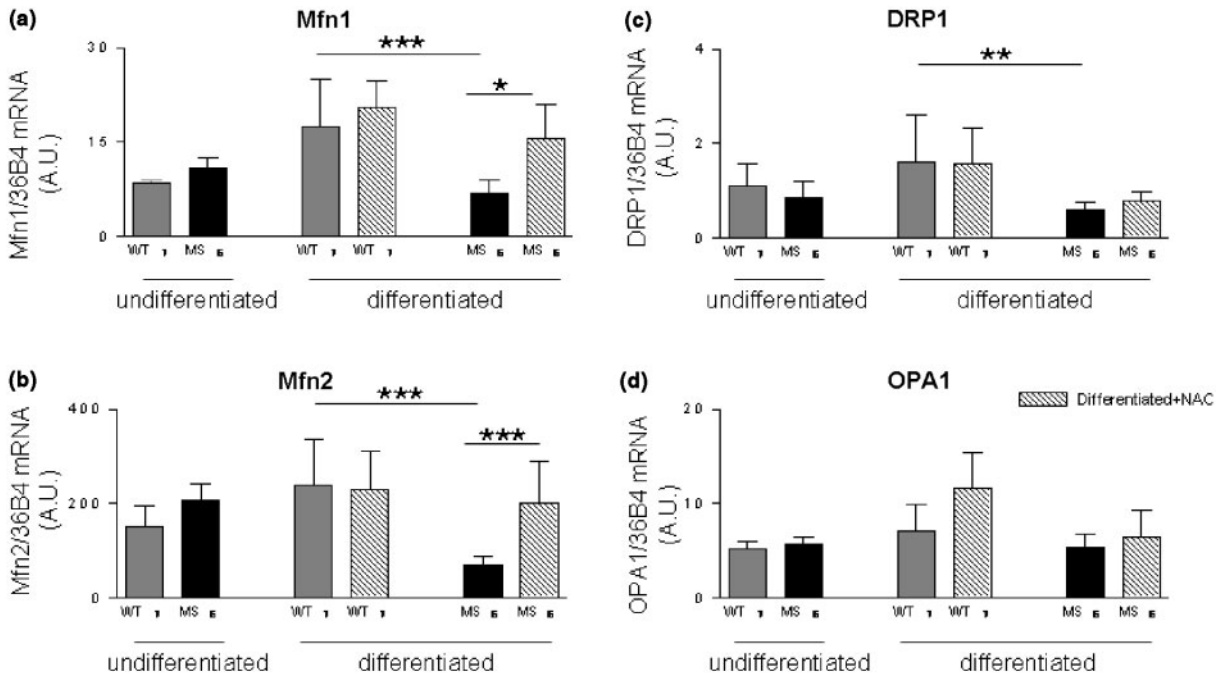

Fig. 5 Altered gene expression of proteins involved in mitochondrial morphology and movement in myotubes with A3243G mtDNA. The level of Mfn1 (**a**), Mfn2 (**b**), DRP1 (**c**) and OPA1 (**d**) were quantified by qPCR in wild-type (WT) and A3243G (MS) undifferentiated and differentiated RD myotubes. Values are expressed as mean ± SD of 3–6 assays carried out in duplicate. Significance: $^{*}P < 0.05$; $^{**}P < 0.01$; $^{***}P < 0.001$.

does not contradict the idea that the enhanced sensitivity of MELAS mitochondria to oxidative stress is relevant to mitochondrial disease. Oxidative stimuli have been shown to induce differentiation of neuronal precursor cells (Tsatmali *et al.*, 2005, 2006) and so ROS homeostasis may play a key role in differentiation. The question therefore arises: is oxidative stress a precursor to, or a consequence of differentiation, or both? In one sense it does not matter whether oxidative stress is a cause or a consequence of differentiation, here the key finding is that oxidative stress occurs in MELAS cybrids, where it produces mitochondrial abnormalities, which are prevented by anti-oxidant treatment; in contrast, there was no evidence of oxidative stress in control cybrids subjected to an identical growth regime. Whilst we cannot be certain that these differences between MELAS and control mitochondria will be recapitulated *in vivo*, they are of potential importance and so worthy of attention, particularly as it is difficult to explain all aspects of mitochondrial disease simply in terms of restricted ATP production.

Others have suggested that elevated ROS is an important factor in the progression of mitochondrial disease (Kirkinezos and Moraes, 2001). *In vitro* (Wong and Cortopassi, 1997) (Pang *et al.*, 2001) and *in vivo* studies (Ohkoshi *et al.*, 1995; Filosto *et al.*, 2002) gave indirect evidence of increased ROS production in association with the A3243G MELAS mutation. Ohkoshi and Filosto observed an increased defense from ROS-mediated injury in ragged-red fibres of MELAS patients. Wong (Wong and Cortopassi, 1997) demonstrated that osteosarcoma cybrids with A3243G mtDNA display heightened sensitivity to H_2O_2; and Pang (Pang *et al.*, 2001) reported enhanced oxidative damage to lipids and DNA in cybrids harbouring >90% A3243G mtDNA. There are also reports of oxidative damage in association with the NARP mutation (Mattiazzi *et al.*, 2004) and LHON mutations (Gonzalo *et al.*, 2005), and the latter are associated with increased ROS in a neuronal cybrid line following differentiation (Wong *et al.*, 2002). Thus there is a considerable body of evidence supporting the notion that ROS generation is an important factor in the pathogenesis of mitochondrial DNA disease.

The marked decrease in GSH in A3243G myotubes reported here is consistent with *in vitro* (Pang *et al.*, 2001) and *in vivo* (Hargreaves *et al.*, 2005) observations of a significant decrease in muscle GSH in mitochondrial myopathy. Although GSH deficiency could in theory result from decreased synthesis due to ATP insufficiency, the positive effect of the anti-oxidant NAC suggests that the decrease in GSH in myotubes with mutant mtDNA is due to direct interaction with ROS or its extensive utilisation in the GPx pathway, which amounts to the same thing.

Mitochondrial morphology and movement involves a large cohort of proteins working in concert (Chan, 2006). Changes in the form or expression of components of this orchestra perturb mitochondrial dynamics and cause mitochondrial accumulation or clustering in the perinuclear region of mammalian cells. Such perturbations include a mutant kinesin protein KIF5B (Tanaka *et al.*, 1998), overexpression of mitofusin 2 (Rojo *et al.*, 2002), down-regulation of OPA1 (Kamei *et al.*, 2005), overexpression of hFis 1 (Frieden *et al.*, 2004) and a mutation in the GTPase domain of DRP1 (Smirnova *et al.*, 1998). Here, we observed a coordinated down-regulation of Mfn1, Mfn2 and DRP1 in myotubes carrying A3243G mtDNA, which can explain the abnormal mitochondrial distribution observed. Hence, mutant mtDNA can be added to the list of factors that can perturb mitochondrial morphology. The observation that NAC restores to normal the mitochondrial network and Mfn1 and Mfn2 mRNA levels suggests that ROS homeostasis plays a critical role in ensuring normal mitochondrial distribution.

Myogenesis requires contact and fusion of individual myoblasts into multinucleate myotubes, a process stimulated by calcium uptake (Shin *et al.*, 1996). The elevation of mitochondrial calcium induces a shift of energy metabolism from glycolytic to aerobic ATP production (Leary *et al.*, 1998; Lyons *et al.*, 2004). Therefore we propose that the shift in energy metabolism that accompanies myogenesis places an intolerable load on mitochondria harbouring A3243G mtDNA. It is known that A3243G mtDNA is associated with decreased OXPHOS capacity (Chomyn *et al.*, 1992), and impaired complex I function in particular (Dundar *et al.*, 1996) Respiratory insufficiency precipitates increased ROS production (Brookes *et al.*, 2004). Hence, the switch to aerobic metabolism upon differentiation will increase dependence on a faltering OXPHOS system, leading to further increases in superoxide production, which overwhelm the cells antioxidant defenses.

Many of the observed mitochondrial abnormalities in differentiated myoblasts with A3243G mtDNA (Figs. 1–5) are not the result of OXPHOS deficiency, but a secondary consequence of increased ROS production, as NAC is an anti-oxidant that does not restore OXPHOS (Fig. 3a, COX). The fact that cultured myotubes with mutant mtDNA develop mitochondrial abnormalities, and that this can be prevented by anti-oxidant treatment, suggests that excess ROS production is a significant contributor to mitochondrial dysfunction. Mouse models are available that develop cytochrome *c* oxidase deficiency and undergo mitochondrial proliferation (Inoue *et al.*, 2000) and so the efficacy of NAC or other anti-oxidants on muscle mitochondria *in vivo* can readily be assessed. Anti-oxidants are not expected to provide a panacea for mitochondrial DNA disorders as they do not address the underlying OXPHOS deficiency, nevertheless they could ameliorate some symptoms and may delay progression of the disease.

Supplementary material

Supplementary material is available at *Brain* online.

Acknowledgements

We thank Dr M. Ceccon for the technical assistance. This work was supported by grants to Lodovica Vergani from Telethon: N° 1252, AFM N° 11032, by grants to Ian Holt from the UK Medical Research Council, the Muscular Dystrophy Campaign and the European Union FP6 integrated programme, Mitocombat and by grants to Aaron Russell from the Fonds National Suisse de la Recherche Scientifique: N° 3200B0-105936/1 and AFM N° 11879.

References

Antonicka H, Sasarman F, Kennaway NG, Shoubridge EA. The molecular basis for tissue specificity of the oxidative phosphorylation deficiencies in patients with mutations in the mitochondrial translation factor EFG1. Hum Mol Genet 2006; 15: 1835–46.

Bach D, Pich S, Soriano FX, et al. Mitofusin-2 determines mitochondrial network architecture and mitochondrial metabolism. A novel regulatory mechanism altered in obesity. J Biol Chem 2003; 278: 17190–7.

Brookes PS, Yoon Y, Robotham JL, Anders MW, Sheu SS. Calcium, ATP, and ROS: a mitochondrial love-hate triangle. Am J Physiol Cell Physiol 2004; 287: C817–33.

Chan DC. Mitochondria: dynamic organelles in disease, aging, and development. Cell 2006; 125: 1241–52.

Chomyn A, Enriquez JA, Micol V, Fernandez-Silva P, Attardi G. The mitochondrial myopathy, encephalopathy, lactic acidosis, and stroke-like episode syndrome-associated human mitochondrial tRNALeu(UUR) mutation causes aminoacylation deficiency and concomitant reduced association of mRNA with ribosomes. J Biol Chem 2000; 275: 19198–209.

Chomyn A, Martinuzzi A, Yoneda M, et al. MELAS mutation in mtDNA binding site for transcription termination factor causes defects in protein synthesis and in respiration but no change in levels of upstream and downstream mature transcripts. Proc Natl Acad Sci USA 1992; 89: 4221–5.

Dunbar DR, Moonie PA, Jacobs HT, Holt IJ. Different cellular backgrounds confer a marked advantage to either mutant or wild-type mitochondrial genomes. Proc Natl Acad Sci USA 1995; 92: 6562–6.

Dunbar DR, Moonie PA, Zeviani M, Holt IJ. Complex I deficiency is associated with 3243G:C mitochondrial DNA in osteosarcoma cell cybrids. Hum Mol Genet 1996; 5: 123–9.

Filosto M, Tonin P, Vattemi G, Spagnolo M, Rizzuto N, Tomelleri G. Antioxidant agents have a different expression pattern in muscle fibers of patients with mitochondrial diseases. Acta Neuropathol (Berl) 2002; 103: 215–20.

Finkel T. Oxidant signals and oxidative stress. Curr Opin Cell Biol 2003; 15: 247–54.

Frieden M, James D, Castelbou C, Danckaert A, Martinou JC, Demaurex N. Ca(2+) homeostasis during mitochondrial fragmentation and perinuclear clustering induced by hFis1. J Biol Chem 2004; 279: 22704–14.

Gonzalo R, Garcia-Arumi E, Llige D, et al. Free radicals-mediated damage in transmitochondrial cells harboring the T14487C mutation in the ND6 gene of mtDNA FEBS Lett 2005; 579: 6909–13.

Goto Y, Nonaka I, Horai S. A mutation in the tRNA(Leu)(UUR) gene associated with the MELAS subgroup of mitochondrial encephalomyopathies. Nature 1990; 348: 651–3.

Halliwell B. Oxidative stress in cell culture: an under-appreciated problem? FEBS Lett 2003; 540: 3–6.

Hammans SR, Sweeney MG, Wicks DA, Morgan-Hughes JA, Harding AE. A molecular genetic study of focal histochemical defects in mitochondrial encephalomyopathies. Brain 1992; 115: 343–65.

Hargreaves IP, Sheena Y, Land JM, Heales SJ. Glutathione deficiency in patients with mitochondrial disease: implications for pathogenesis and treatment. J Inherit Metab Dis 2005; 28: 81–8.

Hess JF, Parisi MA, Bennett JL, Clayton DA. Impairment of mitochondrial transcription termination by a point mutation associated with the MELAS subgroup of mitochondrial encephalomyopathies. Nature 1991; 351: 236–9.

Inoue K, Nakada K, Ogura A, et al. Generation of mice with mitochondrial dysfunction by introducing mouse mtDNA carrying a deletion into zygotes. Nat Genet 2000; 26: 176–81.

Jacobs HT. The mitochondrial theory of aging: dead or alive? Aging Cell 2003; 2: 11–7.

Kamei S, Chen-Kuo-Chang M, Cazevieille C, et al. Expression of the Opa1 mitochondrial protein in retinal ganglion cells: its downregulation causes aggregation of the mitochondrial network. Invest Ophthalmol Vis Sci 2005; 46: 4288–94.

Kelly GS. Clinical applications of N-acetylcysteine. Altern Med Rev 1998; 3: 114–27.

King MP, Attardi G. Human cells lacking mtDNA: repopulation with exogenous mitochondria by complementation. Science 1989; 246: 500–3.

Kirkinezos IG, Moraes CT. Reactive oxygen species and mitochondrial diseases. Semin Cell Dev Biol 2001; 12: 449–57.

Kobayashi T, Askanas V, Engel WK. Human muscle cultured in monolayer and cocultured with fetal rat spinal cord: importance of dorsal root ganglia for achieving successful functional innervation. J Neurosci 1987; 7: 3131–41.

Kraft CS, LeMoine CM, Lyons CN, Michaud D, Mueller CR, Moyes CD. Control of mitochondrial biogenesis during myogenesis. Am J Physiol Cell Physiol 2006; 290: C1119–27.

Leary SC, Battersby BJ, Hansford RG, Moyes CD. Interactions between bioenergetics and mitochondrial biogenesis. Biochim Biophys Acta 1998; 1365: 522–30.

Leger B, Vergani L, Soraru G, et al. Human skeletal muscle atrophy in amyotrophic lateral sclerosis reveals a reduction in Akt and an increase in atrogin-1. FASEB J 2006; 20: 583–5.

Lyons CN, Leary SC, Moyes CD. Bioenergetic remodeling during cellular differentiation: changes in cytochrome c oxidase regulation do not affect the metabolic phenotype. Biochem Cell Biol 2004; 82: 391–9.

Mattiazzi M, Vijayvergiya C, Gajewski CD, et al. The mtDNA T8993G (NARP) mutation results in an impairment of oxidative phosphorylation that can be improved by antioxidants. Hum Mol Genet 2004; 13: 869–79.

Moraes CT, Ricci E, Bonilla E, DiMauro S, Schon EA. The mitochondrial tRNA(Leu(UUR)) mutation in mitochondrial encephalomyopathy, lactic acidosis, and strokelike episodes (MELAS): genetic, biochemical, and morphological correlations in skeletal muscle. Am J Hum Genet 1992; 50: 934–49.

Morgan-Hughes JA, Sweeney MG, Cooper JM, et al. Mitochondrial DNA (mtDNA) diseases: correlation of genotype to phenotype. Biochim Biophys Acta 1995; 1271: 135–40.

Ohkoshi N, Mizusawa H, Shiraiwa N, Shoji S, Harada K, Yoshizawa K. Superoxide dismutases of muscle in mitochondrial encephalomyopathies. Muscle Nerve 1995; 18: 1265–71.

Pang CY, Lee HC, Wei YH. Enhanced oxidative damage in human cells harboring A3243G mutation of mitochondrial DNA: implication of oxidative stress in the pathogenesis of mitochondrial diabetes; 2001. pp. S45–56.

Pletjushkina OY, Lyamzaev KG, Popova EN, et al. Effect of oxidative stress on dynamics of mitochondrial reticulum. Biochim Biophys Acta 2006; 1757: 518–24.

Rojo M, Legros F, Chateau D, Lombes A. Membrane topology and mitochondrial targeting of mitofusins, ubiquitous mammalian homologs of the transmembrane GTPase Fzo. J Cell Sci 2002; 115: 1663–74.

Saada A, Shaag A, Elpeleg O. mtDNA depletion myopathy: elucidation of the tissue specificity in the mitochondrial thymidine kinase (TK2) deficiency. Mol Genet Metab 2003; 79: 1–5.

Schafer FQ, Buettner GR. Redox environment of the cell as viewed through the redox state of the glutathione disulfide/glutathione couple. Free Radic Biol Med 2001; 30: 1191–212.

Shin KS, Park JY, Ha DB, Chung CH, Kang MS. Involvement of K(Ca) channels and stretch-activated channels in calcium influx, triggering membrane fusion of chick embryonic myoblasts. Dev Biol 1996; 175: 14–23.

Smirnova E, Shurland DL, Ryazantsev SN, van der Bliek AM. A human dynamin-related protein controls the distribution of mitochondria. J Cell Biol 1998; 143: 351–8.

Tanaka Y, Kanai Y, Okada Y, et al. Targeted disruption of mouse conventional kinesin heavy chain, kif5B, results in abnormal perinuclear clustering of mitochondria. Cell 1998; 93: 1147–58.

Taylor RW, Turnbull DM. Mitochondrial DNA mutations in human disease. Nat Rev Genet 2005; 6: 389–402.

Tiranti V, Munaro M, Sandona D, et al. Nuclear DNA origin of cytochrome c oxidase deficiency in Leigh's syndrome: genetic evidence based on patient's-derived rho degrees transformants. Hum Mol Genet 1995; 4: 2017–23.

Tsatmali M, Walcott EC, Crossin KL. Newborn neurons acquire high levels of reactive oxygen species and increased mitochondrial proteins upon differentiation from progenitors. Brain Res 2005; 1040: 137–50.

Tsatmali M, Walcott EC, Makarenkova H, Crossin KL. Reactive oxygen species modulate the differentiation of neurons in clonal cortical cultures. Mol Cell Neurosci 2006; 33: 345–57.

van den Ouweland JM, Lemkes HH, Ruitenbeek W, et al. Mutation in mitochondrial tRNA(Leu)(UUR) gene in a large pedigree with maternally transmitted type II diabetes mellitus and deafness. Nat Genet 1992; 1: 368–71.

Van Heerebeek L, Meischl C, Stooker W, Meijer CJ, Niessen HW, Roos D. NADPH oxidase(s): new source(s) of reactive oxygen species in the vascular system? J Clin Pathol 2002; 55: 561–8.

Vergani L, Floreani M, Russell A, et al. Antioxidant defences and homeostasis of reactive oxygen species in different human mitochondrial DNA-depleted cell lines. Eur J Biochem 2004; 271: 3646–56.

Vergani L, Prescott AR, Holt IJ. Rhabdomyosarcoma rho(0) cells: isolation and characterization of a mitochondrial DNA depleted cell line with 'muscle-like' properties. Neuromuscul Disord 2000; 10: 454–9.

Wittenhagen LM, Kelley SO. Dimerization of a pathogenic human mitochondrial tRNA. Nat Struct Biol 2002; 9: 586–90.

Wong A, Cavelier L, Collins-Schramm HE, et al. Differentiation-specific effects of LHON mutations introduced into neuronal NT2 cells. Hum Mol Genet 2002; 11: 431–8.

Wong A, Cortopassi G. mtDNA mutations confer cellular sensitivity to oxidant stress that is partially rescued by calcium depletion and cyclosporin A. Biochem Biophys Res Commun 1997; 239: 139–45.

Yasukawa T, Kirino Y, Ishii N, et al. Wobble modification deficiency in mutant tRNAs in patients with mitochondrial diseases. FEBS Lett 2005; 579: 2948–52.

Yasukawa T, Suzuki T, Ueda T, Ohta S, Watanabe K. Modification defect at anticodon wobble nucleotide of mitochondrial tRNAs(Leu)(UUR) with pathogenic mutations of mitochondrial myopathy, encephalopathy, lactic acidosis, and stroke-like episodes. J Biol Chem 2000; 275: 4251–7.